JOURNAL OF APPLIED ELECTROCHEMISTRY **16** (1986) 291–303

Secondary current distribution in a two-dimensional model cell composed of an electrode with an open part

YOSHINORI NISHIKI

Research and Development Center, Permelec Electrode Ltd., 1159, Ishikawa, Fujisawa, Kanagawa prefecture, 252 Japan

KOICHI AOKI, KOICHI TOKUDA, HIROAKI MATSUDA

Department of Electronic Chemistry, Graduate School at Nagatsuta, Tokyo Institute of Technology, Nagatsuta, Midori-ku, Yokohama, 227 Japan

Received 2 January 1985; revised 17 May 1985

On the assumption that the relation between the overpotential and the current density is expressed by linear and Butler–Volmer equations, secondary current distributions were obtained in a two-dimensional model cell in which a working electrode with an open part serving to release gas bubbles to the back side of the electrode is located parallel to a counter electrode or a separator. Cell resistances or cell voltage in the model cell were evaluated for various combinations of geometrical parameters and heterogeneous kinetic parameters by means of the finite element method. As a result, when the kinetic equation was the linear approximation, the cell resistance or cell voltage varied mainly with two geometrical parameters (the interelectrode distance and the electrode surface ratio) and the kinetic parameters. On the other hand, when the kinetic equation was of the Butler–Volmer type the cell voltage varied with the kinetic parameters and the percentage of open area instead of the electrode surface ratio. In order to facilitate estimation of cell voltage for an industrial production-type cell composed of electrodes with voids or holes, the computed cell voltages were expressed as functions of these parameters in simple approximate equations. A criterion for estimating whether the cell voltage is controlled by the overpotential or the ohmic drop is presented.

Nomenclature

a	linear overpotential coefficient, given by Equation 7
B_a	coefficient defined by Equation 23
B_b	coefficient defined by Equation 24
b	linear overpotential coefficient given by Equation 7
d_1	distance between the front side of the working electrode and the separator (or the counter electrode when cell has no separator)
d_2	thickness of the separator
V_{eq}	open circuit potential difference between working and counter electrodes
F	Faraday constant
I	total current per half pitch
i	current density at the working electrode
i_0	exchange current density
n	number of electrons transferred in the electrode reaction
o_p	percentage of open area, given by Equation 2 for the present model
p	pitch, i.e. twice the length of the unit cell, defined by 2(BC) in Fig. 2
R	gas constant
r	unit-cell resistance, defined by Equation 33
r_{rs}	residue of r from sum of r_0 and r_η
r_0	ohmic resistance of the solution when $o_p = 0$
r_0'	ohmic resistance in the model cell estimated from Equations 37 and 38
r_η	resistance due to the overpotential when $o_p = 0$
r_η'	resistance due to the overpotential in the

0021–891X/86 $03.00 + .12

model cell estimated from Equations 37 and 38

s electrode surface ratio or superficial surface area, given by Equation 3 for the present model

T absolute temperature

t thickness of the working electrode, defined by EF in Fig. 2

u_k function defined by Equation 14

v weight function

V cell voltage

w width of the working electrode, defined by 2(DE) in Fig. 2

x abscissa located on the cell model

y ordinate located on the cell model

α anodic transfer coefficient

β linear overpotential kinetic parameter, defined by Equation 18

dy infinitesimal length on the boundary

ζ dimensionless cell voltage, defined by Equation 20

η overpotential at the working electrode

θ Butler–Volmer overpotential kinetic parameter at parallel plate electrode, defined by Equation 29

θ' Butler–Volmer overpotential kinetic parameter in the model cell, defined by Equation 45

Λ Butler–Volmer overpotential kinetic parameter, defined by Equation 19

v coordinate perpendicular to the boundary of the model cell

ξ logarithm of $(I/i_0)/(p/2)$, defined by Equation 28

ϱ_1 resistivity of the solution phase

ϱ_2 resistivity of the separator

ϕ potential in the cell

ϕ' normalized potential, given by Equation 15

ϕ_c inner potential in the solution at the side of the counter electrode

ϕ_w inner potential in the solution at the side of the working electrode

ϕ'_w normalized inner potential in the solution at the side of the working electrode, defined by Equation 21

χ ratio of the overpotential to the ohmic drop

Γ double integration space in the solution or the separator phase

Subscripts

k solution (k = 1) or separator (k = 2)

c counter electrode

w working electrode

1. Introduction

In the design of industrial production-type cells, effort is made to minimize ohmic drop in the cell by considering several kinds of cell configuration. If electrodes have voids or holes through which solution and evolving gas bubbles pass in order to be removed from the interelectrode space, it is difficult to estimate ohmic drop by a simple algebraic calculation because current is distributed not only in the interelectrode space but also in the voids and at the back of the electrode. In a previous paper [1], current distribution at such an electrode with voids was obtained theoretically on the basis of a simple cell model with no overpotential. In real industrial cells, however, overpotential also has to be taken into consideration.

The current distribution associated with the overpotential, i.e. the secondary current distribution, has been theoretically studied on simple cell configurations by Kasper [2–4], Wagner [5, 6], Ishizaka and Matsuda [7–10] and Tobias [11] for the case of linear overpotential–current density relationships. It is difficult to obtain analytical solutions for the secondary current distribution when the overpotential has a non-linear relation to the current density, e.g. via Tafel or Butler–Volmer equations. When overpotential was expressed by the Tafel equation, Ishizaka and Matsuda also derived analytical solutions of the secondary current distribution in simple forms of cell configuration by use of Fourier expansions [7–10]. For complex cell configurations, numerical computation is a poweful tool. Alkire *et al.* [12] applied the finite element method to predicting electrode shape change at a cathode during electrodeposition and obtained the secondary potential field distribution obeying the Butler–Volmer kinetic equation in a rectangular cell. Sautebin *et al.* [13] applied the

finite element method to the simulation of the levelling of a triangular surface during anodic dissolution in electrochemical machining.

The goal of this investigation is to evaluate the secondary current distribution in the model cell composed of an electrode with voids. The relation between the overpotential and the current density treated here obeys linear and Butler–Volmer equations. The former relation is selected on the basis that over a restricted potential region, the general overpotential–current density relation may be linearized. The latter involves the well-known Tafel equation as a limiting case for sufficiently large overpotential. The computational method employed is the finite element method.

2. Computation

We assume that

(a) the solution and the separator have uniform resistivities over each phase;

(b) the resistances of the working and the counter electrodes are small enough to be negligible in comparison with those of the solution and the separator, so that potential is distributed only in the solution and in the separator;

(c) the electrolyte is of uniform constitution;

(d) the relations between the overpotential and the current density at the working electrode are expressed either by linear or Butler–Volmer equations;

(e) there is no overpotential at the counter electrode;

(f) concentration variation is neglected.

On these assumptions, a scheme of potential distribution in a one-dimensional cell with parallel plate electrodes is illustrated in Fig. 1 when a constant current is flowing in the cell with and without overpotential. Taking into account that the net voltage is $V - V_{eq}$ and that the ohmic drop is given by $\phi_w - \phi_c$, we can express the overpotential as

$$\eta = V - V_{eq} - (\phi_w - \phi_c) \tag{1}$$

The model cell analysed here is depicted in Fig. 1 of [1] or Fig. 2. The geometrical characteristics of the cell are the interelectrode distance $d_1 + d_2$, the pitch p, the percentage of open area o_p and the electrode surface ratio s, the last two of which are defined by

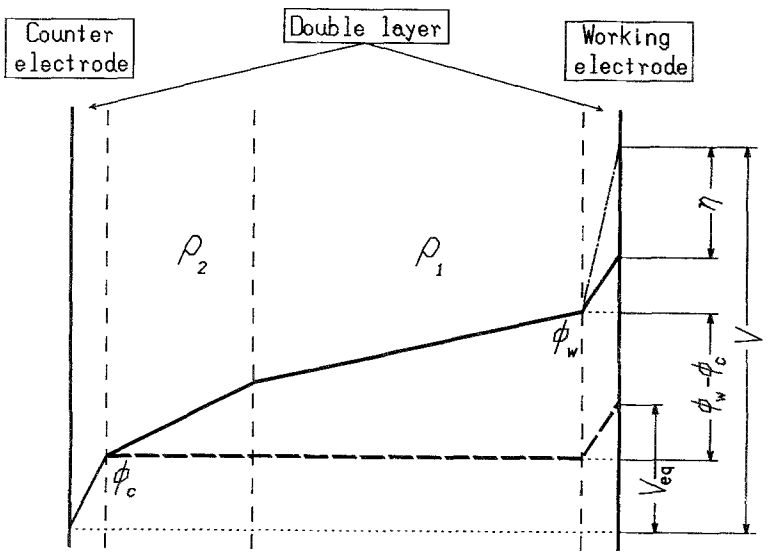

Fig. 1. Scheme of potential distribution in a cell with parallel plate electrodes in galvanostatic electrolysis. The dashed lines represent potential distribution at open circuit. When current is passed through the cell, the distribution is expressed by the solid line without overpotential and by the line (–·–·–) with overpotential.

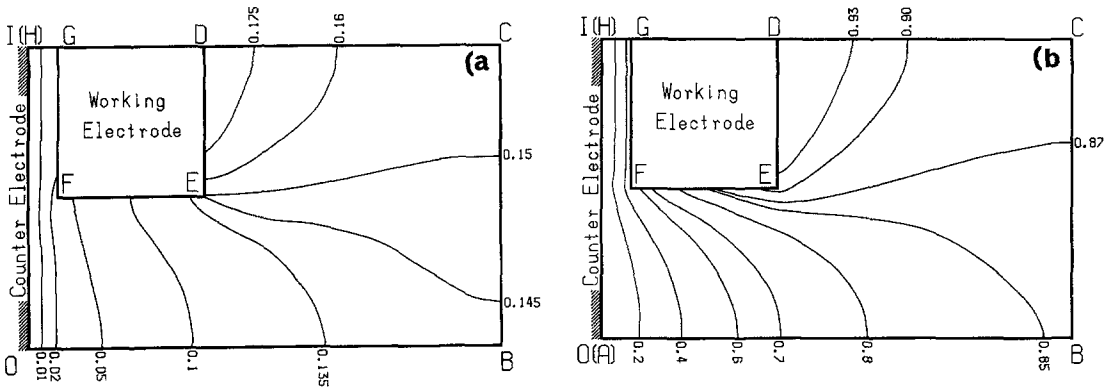

Fig. 2. Potential distributions in the cell with the following parameters: $d_1/p = 0.05$, $o_p = 50\%$, and $s = 1.5$ when the overpotential is of the Butler–Volmer type with the parameters $\zeta = 3.89$, $\alpha = 0.5$ and $\Lambda = 0.195$ for Fig. 2a and $\Lambda = 19.5$ for Fig. 2b. Numbers denote values of $\phi'(=(\phi - \phi_c)/(V - V_{eq}))$.

$$o_p = 100(p - w)/p \tag{2}$$

$$s = 2(w + t)/p \tag{3}$$

The inner potential, ϕ, in the solution and a separator satisfies the two-dimensional Laplace equation given by

$$\partial^2\phi/\partial x^2 + \partial^2\phi/\partial y^2 = 0 \tag{4}$$

The inner potentials on the sides of the working and the counter electrodes are taken to be ϕ_w and ϕ_c, respectively, i.e.

$$\phi = \phi_w \quad \text{on the sides DEFG} \tag{5}$$

$$\phi = \phi_c \quad \text{on the side OI} \tag{6}$$

ϕ_c has a constant value on OI because of assumption (e). On the contrary, ϕ_w varies with position on the side DEFG and hence it is an unknown function to be solved in this calculation. The following two types of overpotential are dealt with here:

$$\eta = a + bi \quad \text{(linear overpotential)} \tag{7}$$

$$i/i_0 = \exp[(\alpha nF/RT)\eta] - \exp\{[(\alpha - 1)nF/RT]\eta\} \quad \text{(Butler–Volmer overpotential)} \tag{8}$$

The current density at the working electrode is given by

$$i = (\partial\phi_1/\partial v)/\varrho_1 \quad \text{on the sides DEFG} \tag{9}$$

Since there is no sink or source of current at the interface AH, between the separator and the solution, the current density in the solution is equal to that in the separator at the interface, i.e.

$$(\partial\phi_1/\partial x)/\varrho_1 = (\partial\phi_2/\partial x)/\varrho_2 \quad \text{on the side AH} \tag{10}$$

Potentials in both the phases at the interface are equal, and hence

$$\phi_1 = \phi_2 \quad \text{on the side AH} \tag{11}$$

On the sides of the insulated walls, the potential gradient is zero, i.e.

$$\partial\phi/\partial v = 0 \quad \text{on the sides OB, BC, CD and GI} \tag{12}$$

We solve the boundary value problem expressed by Equations 4–12 using the conventional finite

element method [14], as has been done previously [1]. Multiplying Equation 4 by a weight function, $v = v(x, y)$, integrating the resulting equation over the solution or the separator phase by application of Green's theorem, inserting the boundary conditions given in Equations 9 and 12 into the resulting equation and eliminating $\partial\phi_1/\partial x$ and $\partial\phi_2/\partial x$ on the side AH by the use of Equation 10, we obtain

$$\varrho_1 \int_{\mathrm{DEFG}} iv\mathrm{d}\gamma + (\varrho_1/\varrho_2) \int_{\mathrm{IO}} (\partial\phi_2/\partial v)v\mathrm{d}\tau = u_1 + u_2(\varrho_1/\varrho_2) \tag{13}$$

with

$$u_k = \iint_{\Gamma_k} [(\partial\phi_k/\partial x)(\partial v/\partial x) + (\partial\phi_k/\partial y)(\partial v/\partial y)]\mathrm{d}x\mathrm{d}y \tag{14}$$

We introduce the dimensionless potential, ϕ', given by

$$\phi' = (\phi - \phi_c)/(V - V_{eq} - a) \tag{15}$$

Substituting Equation 15 into Equations 13 and 14 and replacing i by Equations 7 and 8 yields for linear overpotential

$$[2/(\beta p)] \int_{\mathrm{DEFG}} (1 - \phi'_w)v\mathrm{d}\gamma + (\varrho_1/\varrho_2) \int_{\mathrm{IO}} (\partial\phi'_2/\partial v)v\mathrm{d}\gamma = u'_1 + u'_2(\varrho_1/\varrho_2) \tag{16}$$

and for Butler–Volmer overpotential

$$[2\Lambda/(\zeta p)] \int_{\mathrm{DEFG}} \{\exp[\alpha\zeta(1 - \phi'_w)] - \exp[(\alpha - 1)\zeta(1 - \phi'_w)]\}v\mathrm{d}\tau + (\varrho_1/\varrho_2) \int_{\mathrm{IO}} (\partial\phi'_2/\partial v)v\mathrm{d}\tau = u'_1 + u'_2(\varrho_1/\varrho_2) \tag{17}$$

where

$$\beta = b/[\varrho_1(p/2)] \quad \text{(for the linear relation)} \tag{18}$$

$$\Lambda = [nFi_0\varrho_1(p/2)]/RT \quad \text{(for the Butler–Volmer equation)} \tag{19}$$

$$\zeta = nF(V - V_{eq})/RT \quad \text{(for the Butler–Volmer equation)} \tag{20}$$

$$\phi'_w = (\phi_w - \phi_c)/(V - V_{eq} - a) \tag{21}$$

It is ϕ'_w that is to be obtained in this calculation. Function u'_k ($k = 1, 2$) in Equations 16 and 17 corresponds to u_k in Equation 14 in which ϕ is replaced by ϕ'. The parameters for the Butler–Volmer equations are not only Λ but also α. When η is so small that the exponential in the Butler–Volmer equation can be approximated as a linear dependence [15], Λ^{-1} is equal to β.

Equations 16 and 17 were discretized into square elements with the same size and were inverted into an equivalent matrix formula involving the Dirichlet conditions $\phi' = 0$ on the side OI. The interpolation function employed was a linear function. Detailed procedures of the discretization and the matrix formulation have been described previously [1]. Since Equation 16 has the same form as in equation 11 of [1] it was solved by the method previously described [1]. A set of the simultaneous equations corresponding to Equation 17, however, contains a nonlinear component in the first terms. If we apply the Newton method to Equation 17, we obtain

$$(2\Lambda/\zeta p) \int_{\mathrm{DEFG}} \{B_a - B_b - [B_a/\alpha - B_b/(\alpha - 1)][\phi'^{(k)}_w - \phi'^{(k-1)}_w]/\zeta\}v\mathrm{d}\gamma + (\varrho_1/\varrho_2) \int_{\mathrm{IO}} (\partial\phi'^{(k)}_2/\partial v)v\mathrm{d}\gamma = u'^{(k)}_1 + (\varrho_1/\varrho_2)u'^{(k)}_2 \tag{22}$$

with

$$B_a = \exp[\alpha\zeta(1 - \phi'^{(k-1)}_w)] \tag{23}$$

$$B_b = \exp[(\alpha - 1)\zeta(1 - \phi'^{(k-1)}_w)] \tag{24}$$

where $\phi_w'^{(k)}$ denotes a value of ϕ_w' at the k-th iteration. Since Equation 22 is linear with respect to $\phi_w'^{(k)}$, it is possible to obtain sucessively $\phi_w'^{(k)}$ from known values of $\phi_w'^{(k-1)}$ by a conventional method providing that the initial potential distribution, $\phi_w'^{(0)}$, is adequately selected. The assembled global matrices for Equation 22 are banded but they are asymmetric because of $\phi_w'^{(k)}$. Hence whole elements in the banded domain, the number of which is twice as many as the numbers of elements frequently employed for banded and symmetrical matrices, were loaded in computer memories. The initial distribution, $\phi_w'^{(0)}$, was taken uniformly to be unity. Starting at the initial value, successively iterated computation was made until convergence was achieved. The typical number of iterations was four. The maximum number of nodal points used was 2500. The total current, I, i.e. the sum of the current densities at all nodes of the boundary, DEFG is expressed by

$$I = \int_{DEFG} (\delta\phi_1/\delta\nu)\mathrm{d}\gamma/\varrho_1 \tag{25}$$

Integration of Equation 25 was performed by Simpson's $\frac{1}{3}$ rule.

3. Relative contribution of overpotential and ohmic drop at parallel plate electrodes

It is of great importance to know the relative contribution of the overpotential and the ohmic drop to the total cell voltage. Since current distributions in two- and three-dimensional cells vary with overpotential, it is difficult to specify the relative contribution. Conversely, the contribution can readily be evaluated in the one-dimensional cell because the current line is unique. Before considering the complicated contribution in the two-dimensional cell, the contribution in the one-dimensional cell is treated here. The relative contribution can be expressed by the ratio, χ, of the overpotential to the ohmic drop. In the one-dimensional cell, χ is given by

$$\chi = r_\eta/r_0 = \eta/[I(\varrho_1 d_1 + \varrho_2 d_2)/(p/2)] \tag{26}$$

Then, this quantity is equivalent to the Wagner number. In the cell with non-uniform current distribution, values of χ are different from those of the Wagner number. For linear overpotential, χ can be expressed as a simple algebraic form. However, χ for Butler–Volmer overpotential varies intricately with current. In order to facilitate understanding of the current–potential characteristics in the two-dimensional model cell, we discuss the dependence of χ on the kinetic parameters at parallel plate electrodes.

Eliminating η from Equations 8 and 26 yields

$$e^\xi = \exp[(\chi)e^{\xi+\theta}] - \exp[(\chi)(1 - 1/\alpha)e^{\xi+\theta}] \tag{27}$$

where

$$\xi = \ln[(I/i_0)/(p/2)] \tag{28}$$

$$\theta = \ln[(\alpha nFi_0(\varrho_1 d_1 + \varrho_2 d_2)/RT] \tag{29}$$

At $\alpha = 0.5$, Equation 27 can be solved with respect to θ as follows:

$$\theta = -\ln(\chi) - \xi + \ln\{\ln[e^\xi/2 + (e^{2\xi}/4 + 1)^{1/2}]\} \tag{30}$$

When the overpotential is of the Tafel type, Equation 30 becomes

$$\theta = -\ln(\chi) - \xi + \ln(\xi) \tag{31}$$

When η is so small that the Butler–Volmer equation can be linearized, Equation 30 becomes

$$\theta = -\ln(\chi) - 0.731 \tag{32}$$

In Fig. 3, curves calculated from Equation 30 for $\chi = 10$ and 0.1 are shown in solid curves, indicating three domains in the $\theta - \xi$ plane. In domain A, the ohmic drop predominates in the cell voltage, while in domain C the overpotential predominates. In intermediate domain B, the cell voltage is controlled by both the ohmic drop and the overpotential. Dotted curves in Fig. 3 were

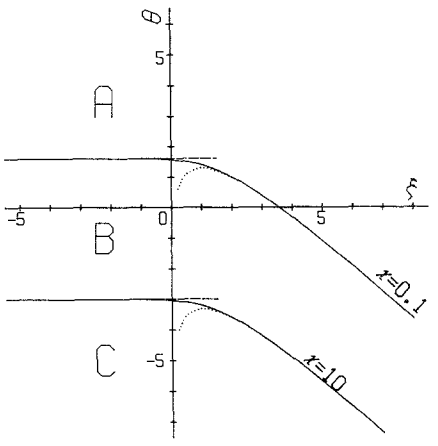

Fig. 3. Diagram of the relation between the Butler–Volmer overpotential and the ohmic drop at parallel plate electrodes. The solid upper and lower curves correspond to $\chi = 0.1$ and 10, respectively. The dotted curves and dashed lines were calculated from Equations 31 and 32, respectively.

calculated from Equation 31 for $\chi = 10$ and 0.1. In the lower and right part of domains B and C the Butler–Volmer equation can be regarded as the Tafel equation. Dashed lines in Fig. 3 were calculated from Equation 32 for $\chi = 10$ and 0.1. In the domain $\xi < 0$, the Butler–Volmer equation can be approximated to the linear relation. When $\theta > 1.6$, the current distribution is primary, regardless of values of ξ. When i or $I/(p/2)$ is sufficiently larger than i_0, the current distribution is still primary even for $\theta < -3.0$. As values of ξ decrease, however, the contribution of the overpotential gradually increases and finally the cell voltage is entirely controlled by the overpotential. This can be explained by the fact that variation of the ohmic drop with I is linear while that of the overpotential is logarithmic.

For electrodes with complicated forms, values of η vary from point to point and, further, it is difficult to determine the characteristic length of the cell. Therefore only the local Wagner number can be determined unequivocally.

4. Results and discussion

4.1. *Potential and current distributions*

Calculated secondary potential distributions in the cell without the separator are shown in Fig. 2 when the overpotential obeys the Butler–Volmer equation. Fig. 2A, which corresponds to the overpotential-controlled case, shows that potential drop in the solution phase plays a minor role in the overall cell voltage when the overpotential is large or the exchange current density is small. One of the significant characteristics of the potential distribution is that the potential of the solution in contact with the working electrode varies from point to point. Consequently the potential is distributed as if equipotential lines might enter in the working electrode. In Fig. 2B, potential distribution is shown for the ohmic drop-controlled case.

In order to examine the current distribution in detail we obtained the secondary current distributions at the working and the counter electrodes, as shown in Fig. 4. When the ratio of the overpotential to the ohmic drop is small (solid curve), corresponding to domain A in Fig. 3, the current concentrates on the FG-side and the confronted part of the counter electrode. For the case of the large ratio of the overpotential to the ohmic drop (dashed curves), corresponding to domain C in Fig. 3, the current density ceases to concentrate at corners E and F and is distributed almost uniformly over the three sides of the working electrode. The current density at the counter electrode facing the open part becomes larger than that at the counter electrode facing the FG-side because the partial current at the former part of the electrode is roughly equal to the sum of the partial currents passing through the DE- and FG-sides, respectively.

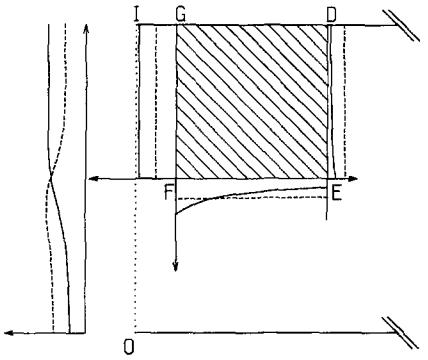

Fig. 4. Current distributions at the working and the counter electrodes when the overpotential is of the Butler–Volmer type with $\zeta = 3.89$ and $\alpha = 0.5$. The solid lines are for a small overpotential $\Lambda = 0.0389$ while the dashed lines are for a large overpotential $\Lambda = 3.89$. The coordinates of the current densities are taken to be perpendicular to the electrode surfaces.

4.2. *Unit-cell resistance or cell voltage*

The cell resistance, r, may be defined by

$$r = (V - V_{eq} - a)/I \tag{33}$$

If a planar working electrode is located parallel to a planar counter electrode, corresponding to the case of $o_p = 0$, all the equipotential lines become straight and parallel and hence the cell resistance can be expressed by simple algebraic sum of the ohmic resistance and the resistance due to the overpotential. This is not the case, however, in the two-dimensional model cell because the shape of current lines in the solution changes depending on the magnitude of overpotential. Since the cell geometry is not simple, it is impossible in principle to specify separately the contributions of the ohmic drop and the overpotential to the whole cell resistance. Nevertheless, the representation of the whole cell resistance in terms of series connections of different kinds of resistance may be helpful for understanding variations of the Wagner number, as discussed in Section 3. In order to pursue this representation, we define two resistances, r_0 and r_η, where r_0 is the ohmic resistance of the solution and the separator which would be observed if a planar working electrode of length $p/2$ (AH-length) were located on FG and on its extended line, i.e. at $o_p = 0$ and r_η is the resistance due to the overpotential in such a case. From these two resistances we can express the whole cell resistance, r, as

$$r = r_0 + r_\eta + r_{rs} \tag{34}$$

where r_{rs} is a residual resistance and varies intricately with the overpotential and cell geometry. We shall describe the dependence of these three resistances on cell geometry and the coefficients of two types of overpotential in the following discussion.

4.2.1. Linear overpotential. r_0 and r_η in this case are simple expressed by $(\varrho_1 d_1 + \varrho_2 d_2)/(p/2)$ and $b/(p/2)\,(=\varrho_1\beta)$, respectively. If these r_0 and r_η terms are inserted into Equation 34, r_{rs} is given by

$$r_{rs} = r - \varrho_1\beta - (\varrho_1 d_1 + \varrho_2 d_2)/(p/2) \tag{35}$$

In Fig. 5, computed values of r_{rs}/ϱ_1 are plotted against β for six values of s. We examined in detail the dependence of r_{rs}/ϱ_1 on the ratio ϱ_2/ϱ_1, four geometrical parameters, d_1/p, d_2/p, o_p and s, and the kinetic parameter β. As a result, we found that r_{rs}/ϱ_1 does not vary appreciably with d_1/p, d_2/p or ϱ_2/ϱ_1 when the following condition holds:

$$d_1/p > 0.3 \tag{36}$$

This fact indicates that most of the variations of r with d_1/p are reflected on r_0. Since condition 36 is frequently fulfilled in real production-type cells with separators, we discuss here the behaviour of

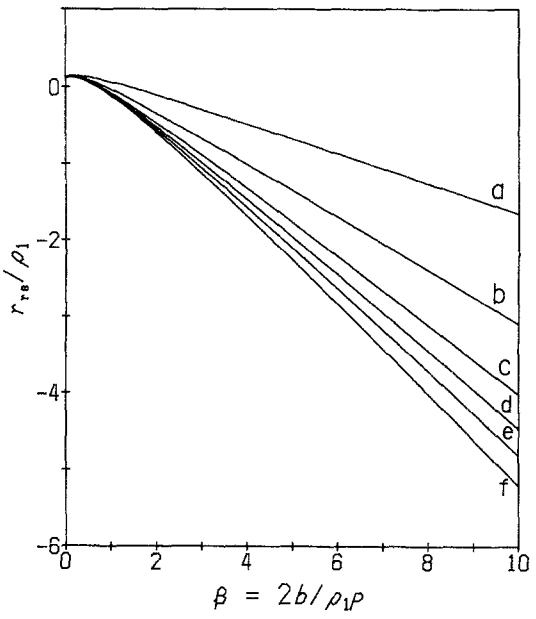

Fig. 5. Variations of $r_{rs}[\varrho_1(p/2)]$ with β for s = (a) 1.2, (b) 1.5, (c) 1.8, (d) 2.0, (e) 2.2 and (f) 2.5 when the overpotential is of the linear type. Geometrical parameters are $o_p = 60\%$, $d_1/p = 0.5$ and $d_2 = 0$.

r_{rs} under this condition. Variations of r_{rs} with o_p can be neglected for $\beta > 2$ while those for $\beta < 0.8$ are slight. Therefore the main factors determining r_{rs} are s and β.

When $\beta < 0.3$, r_{rs} can be regarded as that of the primary current distribution which is expressed by equation 15* of [1]. When values of β exceed 0.6, r_{rs} starts to decrease gradually and then approaches a straight line as shown in Fig. 5. We found that the slope is equal to $(1/s) - 1$. If the overpotential or β is so large that the current distribution at the working electrode is uniform, r varies linearly with the reciprocal of the electrode area. By taking into account the finding that r versus $(p/2)/s$ and r_η versus $p/2$ are both linear, it turns out that r_{rs} varies linearly with $(1/s) - 1$ from the theoretical point of view. On the basis of this linearity, we conclude that the cell resistance is completely controlled by the overpotential when $\beta > 2$. The intermediate region $0.3 < \beta < 2$ is the competitive domain in which both the ohmic drop and the overpotential control the cell voltage.

It may be convenient to have a simple equation that can express the variation of r_{rs} with several parameters. We combined this linearity with equation 15 of [1] valid for extremely small values of β and derived the following approximate equation:

$$r = (\varrho_1 d_1 + \varrho_2 d_2)/(p/2) + \varrho_1 \beta/s + (0.59s - 0.62)(1 - 0.51^\beta)\varrho_1 + 0.333(o_p/100)^{2.1} \times 0.51^\beta \varrho_1 \quad (37)$$

This equation holds for any value of β within 4% of error when $1.5 \leqq s \leqq 2.5$, $o_p \leqq 60\%$ under condition 36. By the use of this equation and known values of several parameters it is possible to evaluate the cell resistance. In Equation 37 the cell resistance cannot be expressed as a simple sum of the terms of the overpotential and the ohmic drop (in contrast with the case at parallel plate electrodes) because r_{rs} largely contributes to the cell voltage.

4.2.2. Butler–Volmer or Tafel overpotential. Since Butler–Volmer overpotential is not proportional to the current density, the total cell resistance is neither inversely proportional to the current under potentiostatic conditions nor proportional to the cell voltage under galvanostatic conditions. For simplicity of the analysis we restrict our attention to galvanostatic or total current controlled

* There was a misprint in equation 15 in [1]. The term $(\varrho_2 d_2 + \varrho_1 d_1)(p/2)$ should be replaced by $(\varrho_2 d_2 + \varrho_1 d_1)/(p/2)$.

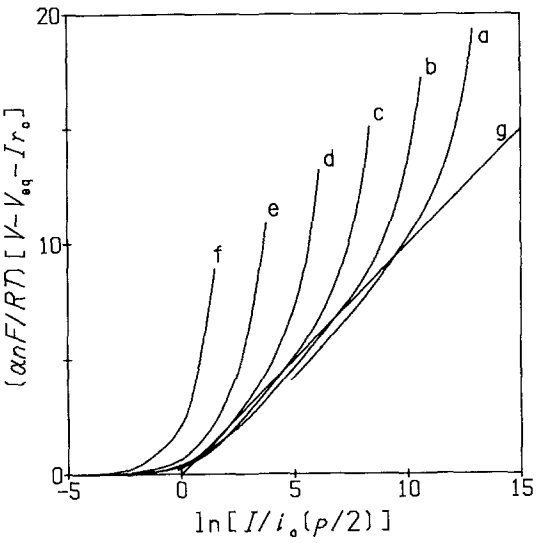

Fig. 6. Dependence of $(\alpha nF/RT)(V - V_{eq} - Ir_0)$ on $\ln\{I/[i_0(p/2)]\}$ computed for several values of $\Lambda = i_0\varrho_1(p/2)nF/RT$: (a), 0.000389; (b), 0.00389; (c), 0.0389; (d), 0.389; (e), 3.89; (f), 38.9, when $\alpha = 0.5$, $o_p = 50\%$, $s = 2$, $d_1/p = 0.5$ and $d_2 = 0$. The straight line represents the Tafel equation when resistivity of the solution is zero.

electrolysis. We carried out the computation of the total current for various combinations of the kinetic and the geometrical parameters under the potentiostatic condition and then regarded $I/[i_0(p/2)]$ as an independent variable. As a dependent variable, we took the apparent overpotential, $(nF/RT)(V - V_{eq} - Ir_0)$, which is defined as the cell voltage from which the ohmic drop, $Ir_0 = I(\varrho_1 d_1 + \varrho_2 d_2)/(p/2)$ at $o_p = 0$, is subtracted. This apparent overpotential equals the product of I by $r_\eta + r_{rs}$ in Equation 34. Then the cell voltage can be expressed by geometrical parameters, mainly o_p, s and $d_1/(p/2)$, and kinetic parameters, α and Λ. In Fig. 6, values of $(\alpha nF/RT)(V - V_{eq} - Ir_0)$ are plotted against $\ln\{I/[i_0(p/2)]\}$ for several values of Λ at $\alpha = 0.5$, $o_p = 50\%$, $s = 2$ and $d_1 = p/2$. The straight line in Fig. 6 is the Tafel line.

For very small values of $\ln[I/i_0(p/2)]$, the overpotential can be regarded as linear overpotential and hence the apparent overpotential is almost zero, consistent with curves for $\beta < 0.5$ in Fig. 5. Since the overpotential hardly contributes to the cell voltage at large values of Λ, e.g. $\Lambda = 39$, the apparent overpotential increases linearly with I, i.e. exponentially with $\ln[I/i_0(p/2)]$. For small values of Λ the apparent overpotential varies along the Butler–Volmer or Tafel line and then increases exponentially. In other words, the cell voltage varies from overpotential-controlled voltage to ohmic drop-controlled when values of $I/i_0(p/2)$ increase. This variation can be visualized if one traces a horizontal line at a value of θ less than -3 in Fig. 3. As values of Λ decrease, the exponentially rising part of the curve only shifts to the right along the Tafel line. The amount of the shift in Fig. 6 is equal to $\ln[I/i_0(p/2)]$ for one decade of Λ.

In order to facilitate estimation of the cell voltage from values of the current flowing, the kinetic parameters and the geometrical cell parameters, we obtained an approximate equation for the cell voltage by examining dependence of the cell voltage on these parameters. The approximate equation thus obtained is

$$\begin{aligned} Ir = V - V_{eq} &= I(\varrho_1 d_1 + \varrho_2 d_2)/(p/2) + (RT/\alpha nF)\ln[I/i_0(p/2)] \\ &+ 0.365\, I\varrho_1 (o_p/100)^{2.1} - RT/2nF \end{aligned} \tag{38}$$

where the error involved in this equation is less than 0.6 for $nF(V - V_{eq})/RT$ under the conditions $0.3 \leqq \alpha \leqq 0.8$, $\Lambda \leqq 0.4$, $\ln[I/i_0(p/2)] \geqq 2$, $1.5 \leqq s \leqq 2.5$, $30\% \leqq o_p \leqq 60\%$ and $d_1/p \geqq 0.1$. The condition $\ln[I/i_0(p/2)] \geqq 2$ corresponds to the Tafel region. Under the condition, $\ln[I/i_0(p/2)] < 0$, the equation for the linear overpotential is valid. Then one can evaluate the cell resistance or the overpotential accurately from Equation 37 instead of Equation 38.

4.3. *Relative contribution of overpotential and ohmic drop in the model cell*

We now demonstrate a criterion to determine whether the cell voltage is controlled by the overpotential or the ohmic drop. The Wagner number is one of the measures of this criterion. However, since η in the model cell varies from point to point, the Wagner number also varies from point to point, being equivocal. Therefore we use for the criterion the ratio, χ, of the overpotential to the ohmic drop.

4.3.1. Linear overpotential. For large values of $\beta(\beta > 2)$, r_{rs} can be separated into the ohmic and the overpotential parts. From Equation 37, it follows that

$$r_0' = (\varrho_1 d_1 + \varrho_2 d_2)/(p/2) + (0.59s - 0.62)\varrho_1 \tag{39}$$

$$r_\eta' = b/[s(p/2)] \tag{40}$$

Then χ is given by

$$\chi = b/[(\varrho_1 d_1 + \varrho_2 d_2)s + (0.59s - 0.62)s\varrho_1(p/2)] \tag{41}$$

χ depends on the electrode surface ratio.

Conversely, for small values of $\beta(\beta < 2)$, it is difficult to separate the cell resistance into r_η' and r_0'. Therefore χ cannot be determined unequivocally.

4.3.2. Butler–Volmer or Tafel overpotential. The term $RT/2nF$ in Equation 38 is much smaller than $V - V_{eq}$ under conventional electrolysis conditions. Then it is possible to roughly separate the terms in Equation 38 into the overpotential and the ohmic drop contributions, respectively:

$$Ir_\eta' = (RT/\alpha nF) \ln [I/i_0(p/2)] \tag{42}$$

$$Ir_0' = I(\varrho_1 d_1 + \varrho_2 d_2)[1 + 0.365(o_p/100)^{2.1}]/(p/2) \tag{43}$$

From Equations 42 and 43, it follows that

$$\theta' = -\ln(\chi) - \xi + \ln(\xi) \tag{44}$$

where

$$\theta' = \ln\{(\alpha nF/RT)i_0(\varrho_1 d_1 + \varrho_2 d_2)[1 + 0.365(o_p/100)^{2.1}]\} \tag{45}$$

Equation 44 has the same form as Equation 31. Thus the curves in Fig. 3 which have been derived for parallel plate electrodes hold also for the case of the two-dimensional model cell if θ is replaced by θ'.

4.4. *Partial currents at three sides of the electrode*

In order to examine dependence of the current distribution at the working electrode on various parameters, it is convenient to take into account the partition of the partial current at DE-, EF- or FG-sides to the total current.

4.4.1. Partial currents for linear overpotential. In Fig. 7, the percentage of partial currents at the three sides are plotted against $\log(\beta)$ for the case of linear overpotential at $o_p = 50\%$ and $s = 1.5$. When β-values increase, the partition at the FG-side decreases while that at the DE-side increases. This variation indicates that the current distribution becomes uniform as the overpotential increases. If the overpotential or β is so large that the distribution is completely uniform, the partition of the current should be equal to the ratio of area of each side to the total area, which is 33.3% for the case in Fig. 7. In this case, the three sides play the same role in electrolysis regardless of values of o_p and s, although the DE-side is located far from the counter electrode.

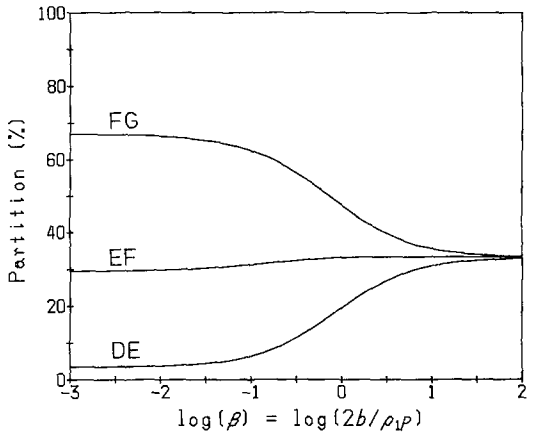

Fig. 7. Variations of partitions of currents at the DE-, EF- and FG-sides with $\log(\beta)$ at $o_p = 50\%$ for the case of linear overpotential when $s = 1.5$, $d_1/p = 0.5$ and $d_2 = 0$.

4.4.2. Partial currents for Butler–Volmer overpotential. In Fig. 8, variations of partitions at the three sides with $\ln[I/i_0(p/2)]$ are shown for five values of Λ. When values of $\ln[I/i_0(p/2)]$ are sufficiently large, the partitions approach 67%, 29% and 4% respectively, for the FG-, EF- and DE-sides, corresponding to the primary current distribution. By taking into account the fact that the ohmic drop varies almost linearly with I while the overpotential follows the logarithmic variation with I, most of the cell voltage for sufficiently large values of $I/i_0(p/2)$ is ascribed to the ohmic drop contribution and hence the current distribution becomes primary.

When values of $\ln[I/i_0(p/2)]$ decrease, the partition at the FG-side decreases and that at the DE-side increases and then they approach constant values depending on Λ-values. These constant values are those of linear overpotential because the Butler–Volmer equation reduces to the linearized equation through the relation $1/\Lambda = \beta$ when $I/i_0(p/2)$ tends to zero. Limiting values of the partition at a small value of $I/i_0(p/2)$ can be found in the curves in Fig. 7. When a Λ-value is more than 10, the current distribution can be regarded as the primary distribution, irrespective of current values. As a Λ-value becomes less than 0.1, curves for the partition shift to the right by an amount $\ln[I/i_0(p/2)]$ for one decade of Λ. This shift corresponds to that of the cell voltage shown in Fig. 6.

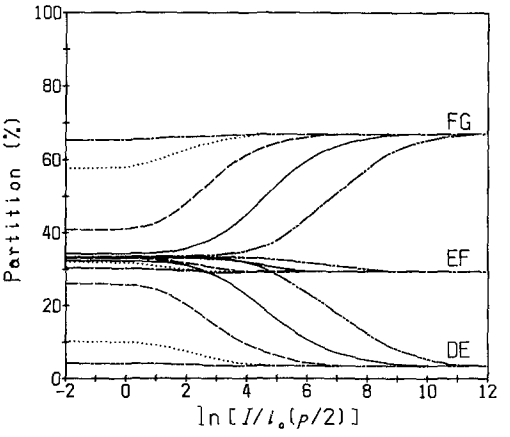

Fig. 8. Variations of partitions of currents at the DE-, EF- and FG-sides with $\ln[I/i_0(p/2)]$ for the case of Butler–Volmer overpotential when values of Λ are: (–··–), 0.00389; (———), 0.0389; (– – –), 0.389; (···), 3.89; (–·–·–), 38.9, calculated for $s = 1.5$, $o_p = 50\%$, $d_1/p = 0.5$ and $d_2 = 0$.

Acknowledgement

The authors wish to express their appreciation of fruitful suggestions by Mr Seiji Nakagawa, President, Permelec Electrode Ltd.

References

[1] Y. Nishiki, K. Aoki, K. Tokuda and H. Matsuda, *J. Appl. Electrochem.* **14** (1984) 653.
[2] C. Kasper, *Trans. Amer. Electrochem. Soc.* **78** (1940) 131.
[3] *Idem, ibid.* **78** (1940) 147.
[4] *Idem, ibid.* **82** (1942) 153.
[5] C. Wagner, *J. Electrochem. Soc.* **98** (1951) 116.
[6] *Idem, ibid.* **99** (1952) 1.
[7] S. Ishizaka and H. Matsuda, *Denkikagaku* **19** (1951) 89.
[8] H. Matsuda and S. Ishizaka, *ibid.* **20** (1952) 38.
[9] *Idem., ibid.* **20** (1952) 84.
[10] S. Ishizaka, H. Matsuda and Y. Wada, *ibid.* **22** (1954) 420.
[11] C. W. Tobias, *J. Electrochem. Soc.* **106** (1959) 833.
[12] R. Alkire, T. Bergh and R. L. Sani, *ibid.* **125** (1978) 1981.
[13] R. Sautebin, H. Froidevaux and D. Landolt, *ibid.* **127** (1980) 1096.
[14] O. C. Zienkiewicz, 'The Finite Element Method', McGraw-Hill, London (1977).
[15] A. J. Bard and L. R. Faulkner, 'Electrochemical methods, Fundamental and Applications', John Wiley, New York (1980) p. 105.